mation is only valid when the diffusion couple lies along an eigenvalue direction. Consequently, the quality of the pseudobinary approximation cannot be reliably estimated because it is impossible to know a priori the directions of the eigenvectors. A promising alternative to experimental measurement of D_{ik} is the use of molecular dynamics simulations that generalize established methods for calculating binary interdiffusion coefficients (*13*).

REFERENCES AND NOTES

1. T. Graham, *Philos. Trans. R. Soc. London* **140**, 1 (1850); A. Fick, *Ann. Phys. (Poggendorf)* **94**, 59 (1855).
2. L. Onsager, *Phys. Rev.* **37**, 405 (1931); *ibid.* **38**, 2265 (1931); _____ and R. M. Fuoss, *J. Phys. Chem.* **36**, 2689 (1932); L. Onsager, *Ann. N.Y. Acad. Sci.* **46**, 241 (1945).
3. Diffusion studies in binary systems involve the determination of a single diffusion coefficient that may be a function of temperature, pressure, and composition. In a ternary system, there are four independent chemical diffusion coefficients; in a quaternary system, nine diffusion coefficients; and, in general, $(n - 1)^2$ diffusion coefficients in an n-component system. Written as a matrix (D_{ik}), the off-diagonal terms (for example, D_{12} and D_{21} in a ternary system) are referred to as the cross-coupling terms because they link the flux of one component to the concentration gradient of a different component.
4. For example, the thermoelectric effect [W. Thomson, *Proc. Roy. Soc. Edinburgh* **3**, 225 (1854)] and the heat conduction in anisotropic solids [G. Stokes, *Camb. Dublin Math J.* **6**, 215 (1851)].
5. Irreversible phenomena as diverse as thermoelectricity, heat conduction in anisotropic materials, thermogalvanomagnetism, isothermal chemical diffusion, and chemical diffusion in a thermal gradient are some notable examples [see S. R. deGroot and P. Mazur, *Non-Equilibrium Thermodynamics* (Dover, New York, 1984); D. D. Fitts, *Nonequilibrium Thermodynamics* (McGraw-Hill, New York, 1962); S. Wisniewski, B. Staniszewski, R. Szymanik, *Thermodynamics of Nonequibirum Processes* (Reidel, Dordrecht, the Netherlands, 1976)]. Experimental data supporting Onsager's approach to these phenomena is summarized in D. G. Miller, *Chem. Rev.* **60**, 15 (1960).
6. For aqueous systems, early attempts to verify the ORR are summarized in D. G. Miller, *J. Phys. Chem.* **63**, 570 (1959). More recently, analysis of the quaternary aqueous system KCl-KH_2PO_4-H_3PO_4 has shown good agreement with the ORR [R. A. Noulty and D. G. Leaist, *ibid.* **91**, 1655 (1987)]. Two useful reviews of metallic alloys are J. S. Kirkaldy, *Adv. Mater. Res.* **4**, 55 (1970) and J. S. Kirkaldy and D. J. Young, *Diffusion in the Condensed State* (Institute of Metals, London, 1987). A more recent verification of the ORR for the Fe-Cr-Al alloy was reported by H. Akuezue and J. Stringer, *Metall. Trans.* **20A**, 2767 (1989). Discussion of organic polymer multicomponent diffusion may be found in a series of papers by W. D. Comper and colleagues [including W. D. Comper, G. J. Checkley, B. N. Preston, *J. Phys. Chem.* **88**, 1068 (1984), and W. D. Comper, P. M. MacDonald, B. N. Preston, *ibid.*, p. 6031].
7. H. Sugawara, K. Nagata, K. Goto, *Metall. Trans. B* **8**, 605 (1977). Note the apparent typographical error in Eqs. 2 and 3 of this reference. The left-hand side should read J_i/ρ instead of J_i where ρ is the melt density.
8. A. K. Varshneya and A. R. Cooper, *J. Am. Ceram. Soc.* **55**, 312 (1972); H. Wakabayashi and Y. Oishi, *J. Chem. Phys.* **68**, 2046 (1978).
9. R. G. Berman and T. H. Brown, *Geochim. Cosmochim. Acta* **48**, 661 (1984). Uncertainties on the Margules parameters are not provided, but relative errors are most likely in the range 5 to 15%.
10. The definition of the diffusive mass flux is deceptively simple: $j_i = \rho w_i(v_i - v)$, where ρ is the density, v_i is the average velocity of component i, and v is the reference velocity. However, the equation of mass conservation (Eq. 2) and the relation between the fluxes and concentration gradients (Eq. 5) must be written differently, depending on the reference velocity used. A number of reference velocities are in common use, including volume, mass, mole, and solvent average velocities. In this report, v is the mass average (or barycentric) velocity.
11. The molar chemical potential for component 1 in a ternary system is given by

$$\tilde{\mu}_1 = \tilde{\mu}^o_1 + RT\ln(x_1) + \tilde{G}^E + x_2\left(\frac{\partial \tilde{G}^E}{\partial x_1}\right)_{x_3} + x_3\left(\frac{\partial \tilde{G}^E}{\partial x_1}\right)_{x_2}$$

where $\tilde{\mu}^o_1$ is the reference state chemical potential, R is the gas constant, x_i is the mole fraction of component i, and $\tilde{G}^E$ is the excess Gibbs free energy of the melt. The chemical potential of components 2 and 3 may be found by permutation of the subscripts. The Margules solution model for the excess Gibbs free energy is

$$\tilde{G}^E = \tilde{W}_{1112}x_1^3x_2 + \tilde{W}_{1122}x_1^2x_2^2 + \tilde{W}_{1222}x_1x_2^3 + \tilde{W}_{1113}x_1^3x_3 + \tilde{W}_{1133}x_1^2x_3^2 + \tilde{W}_{1333}x_1x_3^3 + \tilde{W}_{2223}x_2^3x_3 + \tilde{W}_{2233}x_2^2x_3^2 + \tilde{W}_{2333}x_2x_3^3 + \tilde{W}_{1123}x_1^2x_2x_3 + \tilde{W}_{1223}x_1x_2^2x_3 + \tilde{W}_{1233}x_1x_2x_3^2$$

The Margules parameters are functions of temperature and follow the relation $\tilde{W} = \tilde{W}_H - T\tilde{W}_S$, where H is enthalpy, S is entropy, and the subscripts defining specific component interactions have been dropped for convenience.
12. If the matrix G_{ik} is ill-conditioned (for example, $\det(G_{ik}) = G_{12}G_{21} - G_{11}G_{22}$ is small) the values of L_{ik} will not be accurately determined by Eq. 14. It is still possible to test the validity of the ORR, however. Equating L_{12} and L_{21} leads to the conclusion that the reciprocal relations are valid if $(D_{11}G_{12} - D_{12}G_{11} + D_{21}G_{22} - D_{22}G_{21})$ equals zero. This type of singularity occurs near critical points and is not a problem for the CaO-Al_2O_3-SiO_2 composition under consideration.
13. R. L. Rowley, J. M. Stoker, N. F. Giles, *Int. J. Thermophys.* **12**, 501 (1991).

14. This research was supported by the U.S. Department of Energy (DE-FG03-91ER-14211) and the National Science Foundation (EAR-92-05820). Institute for Crustal Studies contribution 0137-30CM.

21 August 1992; accepted 2 November 1992

Comparative Compressibilities of Silicate Spinels: Anomalous Behavior of $(Mg,Fe)_2SiO_4$

Robert M. Hazen

Compressibilities of five silicate spinels, including γ-Mg_2SiO_4, γ-Fe_2SiO_4, Ni_2SiO_4, and two ferromagnesian compositions, were determined on crystals positioned in the same high-pressure mount. Subjection of all crystals simultaneously to the same pressure revealed differences in compressibility that resulted from compositional differences. Ferromagnesian silicate spinels showed an anomalous 13 percent increase in bulk modulus with increasing iron content, from Mg_2SiO_4 (184 gigapascals) to Fe_2SiO_4 (207 gigapascals). This result suggests that ferrous iron and magnesium, which behave similarly under crustal conditions, are chemically more distinct at high pressures characteristic of the transition zone and lower mantle.

Knowledge of the compression behavior of oxide and silicate minerals helps to reveal the structure and dynamics of the Earth's deep interior. Furthermore, data on these minerals provide an understanding of the varied effects of pressure on structure and bonding. In this report, I describe anomalous compression behavior in ferromagnesian silicate spinels, which are assumed to be major minerals in the Earth's transition zone.

Most crustal minerals, including magnesium-iron silicates, may be modeled as ionic compounds with bond strengths determined to a first approximation by Coulombic forces. In the 1920s, Bridgman first demonstrated empirical inverse correlations between bulk modulus and molar volume and rationalized his results on an electrostatic model (*1*). Relations between bulk modulus and volume have subsequently developed into useful tools to predict properties of oxides, halides, silicates, and many other compounds. Such relations for isomorphous isoelectronic series (*2*), as well as for individual cation coordination polyhedra (*3*), provide a basis for comparison of bulk moduli and individual bond compressibilities throughout a wide range of condensed materials.

The high-pressure behavior of minerals with Mg-Fe^{2+} solid solution has been studied intensively because of the importance of these minerals in models of the Earth. Polymorphs of $(Mg,Fe)SiO_3$ and $(Mg,Fe)_2SiO_4$ are of particular concern because the major element bulk composition of the mantle is believed to fall somewhere between those stoichiometries. A key issue in geophysics and mineral physics has been the nature of the seismic discontinuity at 670 km, which marks the boundary between the transition zone and lower mantle. Both $(Mg,Fe)SiO_3$ silicate perovskite and (Mg,Fe)O are believed to exist below this boundary, whereas $(Mg,Fe)_2SiO_4$ silicate spinel occurs above

Geophysical Laboratory and Center for High-Pressure Research, Carnegie Institution of Washington, Washington, DC 20015–1305.

the discontinuity (*4*). To resolve details of the mineralogy and composition of this region, it is necessary to obtain accurate equations of state of the relevant phases. In particular, an understanding of the effect of the Fe/(Fe+Mg) ratio on mineral properties is essential to determine whether the 670-km feature reflects only a phase change or also compositional boundary (*5, 6*).

In most ferromagnesian minerals, the $Mg\text{-}Fe^{2+}$ substitution has little effect on compressibility (Table 1). Ferrous iron (ionic radius 0.78 Å) is only slightly larger than Mg (ionic radius 0.72 Å) (*7*), so molar volumes of Fe^{2+} end members exceed their Mg counterparts by at most a few percent (Table 1). By the same token, as the systematics of the bulk modulus-volume relation would suggest, compressibilities of Fe^{2+} and Mg end members typically differ by less than a few percent. Only in the cases of wüstite and hercynite, both of which incorporate the smaller, less compressible Fe^{3+} in significant amounts (*8, 9*), is the Fe end member as much as 10% less compressible than the Mg end member.

Table 1. Bulk moduli (K) and molar volumes (V) for end member pairs of ferromagnesian minerals.

Mineral	Composition	K (GPa)	V (cm^3)*	Source
Periclase	MgO	162	11.2	(*8*)
Wüstite	$Fe_{1-x}O$†	145 to 180	12.0 to 12.2	(*8*)
Dolomite	$CaMg(CO_3)_2$	94	64.3	(*25*)
Ankerite	$CaFe(CO_3)_2$	91	65.6	(*25*)
Orthoenstatite	$MgSiO_3$	107	62.7	(*26*)
Orthoferrosilite	$FeSiO_3$	101	65.9	(*27*)
Diopside	$CaMgSi_2O_6$	113	66.0	(*28*)
Hedenbergite	$CaFeSi_2O_6$	120	67.9	(*29*)
Pyrope	$Mg_3Al_2Si_3O_{12}$	173	113.3	(*30*)
Almandine	$Fe_3Al_2Si_3O_{12}$	176	115.4	(*30*)
Spinel	$MgAl_2O_4$	196	39.8	(*31*)
Hercynite	$FeAl_2O_4$†	210	40.8	(*32*)
Forsterite	Mg_2SiO_4	129	43.6	(*33*)
Fayalite	Fe_2SiO_4	132	46.3	(*34*)
Wadsleyite	Mg_2SiO_4	165	40.5	(*11*)
Fe-Wadsleyite	$(Mg_{0.75}Fe_{0.25})_2SiO_4$	170	41.1	(*11*)
Silicate spinel	Mg_2SiO_4	184	39.5	‡
	Fe_2SiO_4	207	42.0	‡

*All molar volumes from (*35*). †Samples of this mineral usually contain significant amounts of Fe^{3+}. ‡This study.

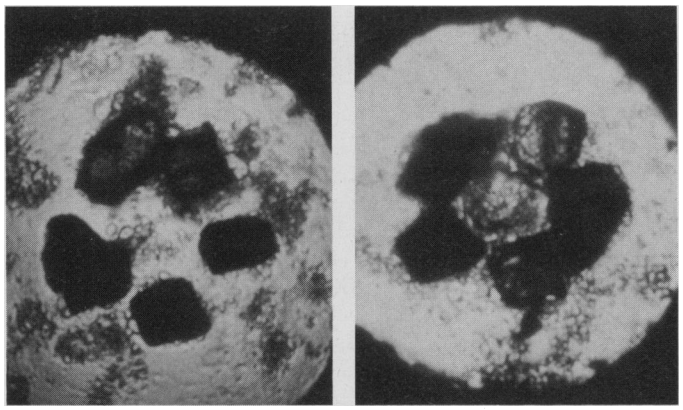

Fig. 1. Two high-pressure diamond-anvil cell mounts containing multiple single crystals of silicate spinel. (**Left**) The first mount, with a gasket hold of 0.50 mm in diameter included end member Mg_2SiO_4 and Ni_2SiO_4 and three crystals of $(Mg,Fe)_2SiO_4$ with Fe/(Mg+Fe) = 0.60, 0.78, and 0.80, respectively. (**Right**) The second mount, with a gasket hole diameter of 0.45 mm, contained Ni and Fe end members and two crystals of Mg_2SiO_4, as well as intermediate Mg-Fe spinels with Fe/(Mg+Fe) = 0.60 (Fe_{60}) and 0.78 (Fe_{78}).

Table 2. Compositions and synthesis conditions of silicate spinel single crystals (*36*).

Composition	Temperature (°C)	Pressure (GPa)	Source and run number
Ni_2SiO_4	1500	7.5	Yagi, Tokyo
Mg_2SiO_4	1400	20.0	Weidner, SUNY #859
$(Fe_{.60}Mg_{.40})_2SiO_4$*	1600	14.5	Ko, SUNY #1013
$(Fe_{.78}Mg_{.22})_2SiO_4$*	1600	12.6	Ko, SUNY #1097
$(Fe_{.80}Mg_{.20})_2SiO_4$*	1610	12.6	Ko, SUNY #1102
Fe_2SiO_4	1400	5.5	Yagi, Tokyo

*Use of ^{57}Fe Mössbauer spectroscopy indicates approximately 5% of total iron as Fe^{3+} in these samples.

High-pressure x-ray diffraction of single crystals in a diamond-anvil pressure cell provides the most accurate method to determine unit-cell volume—typically to a few parts in 10^4. However, comparative studies of pressure-volume trends have been hampered by the difficult goal of pressure measurements below 10 GPa that are better than one or two parts in 10^2. Thus, pressure-volume equations of state are poorly constrained, especially for incompressible crystals such as mantle minerals. One can circumvent this difficulty by mounting several crystals in a single diamond-cell mount with hydrostatic pressure medium (*10, 11*). In this way, relative volumes at several pressures provide an accurate measure of the relative compressibility:

$$\beta_1/\beta_2 \approx [(V_p/V_0)_1 - 1]/[(V_p/V_0)_2 - 1]$$

where β_1 and β_2 are compressibilities of the two crystals and V_0 and V_p are, respectively, the unit-cell volumes measured at room pressure and high pressure. Differences in compressibilities of two crystals as small as 1% have been documented with this equation, although individual compressibilities calculated from the same pressure-volume data may be in error by several percent (*10, 11*).

Magnesium-iron silicate spinel, which is only stable at pressures above ~7 GPa for $\gamma\text{-}Fe_2SiO_4$ to 20 GPa for $\gamma\text{-}Mg_2SiO_4$, has been proposed as a major silicate phase in the Earth's transition zone (*4*). Elasticity or pressure-volume parameters for equations of state have been reported for the Fe end member (*12*), the nickel and cobalt silicate analogs (*13*), and the Mg end member (*14*). No equation-of-state or high-pressure data have appeared for intermediate Mg-Fe silicate spinels, however.

For this study, I obtained single crystals synthesized in large-volume, high-pressure apparatus (Table 2). Samples included end member Ni_2SiO_4, Mg_2SiO_4, and Fe_2SiO_4 spinels, as well as intermediate Mg-Fe silicate spinels with Fe/(Mg+Fe) ratios of 0.60, 0.78, and 0.80 (hereafter referred to as Fe_{60}, Fe_{78}, and Fe_{80}). All crystals were examined first in air by single-crystal x-ray diffraction. Equant crystals no thicker than 60 μm and with good x-ray peak shapes were selected for high-pressure study. The Fe-bearing samples were examined by Mössbauer spectroscopy for Fe^{3+}, a significant component in some silicate spinels (*15*). The Fe end member had no detectable Fe^{3+}, whereas the intermediate Fe_{60} and

Table 3. Unit-cell volumes (Å^3) versus pressure (GPa) for silicate spinel crystals. Data are listed in the order in which they were collected. Uncertainties in last digits are given in parentheses.

Pressure	Ni	Mg		Fe	Fe_{60}	Fe_{78}	Fe_{80}
			Five-spinel mount				
Room *P*, in cell	521.13 (8)	527.10 (8)			546.61 (14)	552.45 (9)	552.89 (19)
2.02 (5)	516.69 (15)	521.47 (8)			541.50 (11)	547.23 (15)	547.74 (18)
3.26 (5)	513.96 (7)	518.10 (27)			538.10 (16)	543.94 (12)	544.52 (10)
			Six-spinel mount				
Room *P*, in cell	521.22 (8)	526.60 (20)*	526.54 (13)†	558.80 (14)	546.42 (12)	552.45 (9)	
4.20 (5)	512.28 (8)	515.33 (13)	515.34 (12)	548.06 (12)	535.68 (8)	541.76 (7)	
2.20 (5)	516.49 (9)	520.43 (13)	520.56 (15)	553.22 (9)	540.75 (8)	546.86 (7)	
0.96 (8)	519.16 (9)	523.77 (19)			544.04 (13)		
0.68 (5)	519.76 (12)	524.65 (11)	524.49 (20)	557.06 (14)	544.67 (16)	550.57 (16)	
4.79 (7)	511.14 (15)	513.85 (13)	513.80 (34)	546.64 (11)	534.37 (7)	540.25 (20)	

*Values in this column are for the first of two crystals of Mg used in the six-spinel mount. †Values in this column are for the second crystal of Mg.

Fe_{78} samples contained approximately 5% of total Fe as Fe^{3+}.

I used crystals up to 100 μm in diameter in two multiple-crystal mounts (*16*). The first mount (Fig. 1) contained five crystals: Mg and Ni end members and the Fe_{60}, Fe_{78}, and Fe_{80} intermediate silicate spinels. Data were collected on all crystals at room pressure and at 2.02 and 3.26 GPa. The second mount had a slightly smaller gasket hole and used six spinel crystals. These crystals were the nickel end member, two crystals of the Mg end member, a crystal of end member γ-Fe_2SiO_4, and the Fe_{60} and Fe_{78} intermediates. Unit-cell parameters of all six crystals were determined (*17*) at five pressures to 4.79 GPa (Table 3).

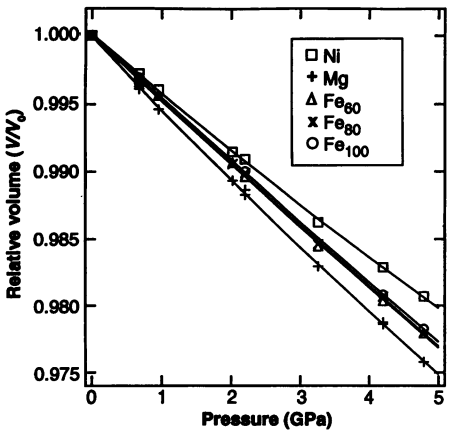

Fig. 2. Relative volumes (V/V_0) versus pressure for five compositions of silicate spinel. The Fe_{80} points include data for both the Fe_{78} and Fe_{80} crystals. The Fe-bearing compositions are significantly less compressible than the Mg end member.

At every pressure, compressibility increased in the order Ni < Fe_{100} < Fe_{80} ≈ Fe_{60} < Mg (Table 4 and Fig. 2). Average relative compressibilities, β_{Mg}/β_x, were 1.25 for Ni_2SiO_4, 1.13 for Fe_2SiO_4, 1.115 for Fe_{80}, and 1.105 for Fe_{60}, all ±0.01. Thus, compressibility of $(Mg,Fe)_2SiO_4$ silicate spinel increased significantly with increasing Fe content.

Pressure-volume data may be fit to a second-order Birch-Murnaghan equation of state, but resulting values for bulk moduli, *K*, are poorly constrained unless V_0 and the pressure derivative of the bulk modulus, *K′*, are fixed (*18*). In the case of γ-Mg_2SiO_4, for example, unconstrained refinement of 11 pressure-volume data yielded a *K* of 183 ± 5 GPa and a *K′* of 6 ± 2. Recent equation-of-state studies of Mg_2SiO_4 (*12*) suggest that *K′* is close to 4.8. With that constraint on the present pressure-volume data, the calculated bulk moduli of the Mg and Ni end members are 184 ± 2 and 233 ± 2 GPa, respectively. These values are close to the previously reported values of 182 ± 1 (*14*) and 226 ± 2 GPa (*13*) for the two compounds, based on Brillouin spectroscopy and powder x-ray diffraction. Bulk moduli of the three Fe-bearing spinels with *K′* constrained to 4.8 are 203 ± 2, 205 ± 2, and 207 ± 3 GPa for Fe_{60}, Fe_{80}, and end member Fe spinels, respectively.

Finite-strain analysis of pressure-volume data emphasizes the compositional effects on both *K* and *K′* (*18*). A plot of Eulerian strain

$$f = [(V/V_0)^{-2/3} - 1]/2$$

versus Birch's normalized pressure,

$$F = P/[3f(1 + 2f)^{2.5}]$$

intersects the *F* axis at the zero-pressure bulk modulus, and the slope indicates deviations of *K′* from a value of 4. Data for Mg silicate spinel, plotted in Fig. 3, suggest that *K′* is slightly greater than 4 and that the bulk modulus is close to 182 GPa, which both agree with earlier work (*14*). In contrast, the pressure-volume data for Ni_2SiO_4 are consistent with *K′* of 4 and bulk modulus of 232 GPa. Data for the three Fe-bearing samples demonstrate that these spinels have bulk moduli significantly greater than that of γ-Mg_2SiO_4. Though slopes of *F* versus *f* curves are subject to large uncertainties, they suggest that *K′* decreases with Fe content to <4 (a value of 3 is consistent with all three Fe-rich compositions). If so, then the difference in bulk moduli of Mg and Fe silicate spinels will be smaller at transition zone pressures.

These data indicate that Mg silicate spinel is approximately 13% more compressible than the Fe^{2+} end member. This difference is significantly larger than has been observed for any other Mg-Fe^{2+} mineral pair and goes against the predictions of bulk modulus-volume systematics. The

Table 4. Relative volumes (V/V_0) versus pressure (GPa) for silicate spinel crystals. Uncertainties in last digits are given in parentheses.

Pressure	Mg #1	Mg #2	Fe_{60}	Fe_{78}	Fe_{80}	Fe	Ni
Room *P*	1.00000	1.00000	1.00000	1.00000	1.00000	1.00000	1.00000
0.68 (5)	0.99631 (20)	0.99611 (36)	0.99680 (36)	0.99660 (30)	—	0.99689 (25)	0.99719 (20)
0.96 (8)	0.99462 (25)	—	0.99564 (28)	—	—	—	0.99604 (16)
2.02 (5)	0.98932 (15)	—	0.99065 (33)	0.99055 (28)	0.9907 (5)	—	0.99148 (25)
2.20 (5)	0.98828 (35)	0.98864 (30)	0.98962 (24)	0.98988 (18)	—	0.99001 (26)	0.99093 (16)
3.26 (5)	0.98293 (40)	—	0.98443 (37)	0.98460 (24)	0.9849 (4)	—	0.98624 (12)
4.20 (5)	0.97860 (35)	0.97873 (23)	0.98034 (24)	0.98065 (18)	—	0.98078 (32)	0.98285 (15)
4.79 (7)	0.97579 (24)	0.9758 (7)	0.97795 (21)	0.97792 (30)	—	0.97824 (30)	0.98067 (20)

question stands: What is the cause of this anomaly?

A partial explanation may lie in the distinctive spinel structure, which features edge-sharing (Mg, Fe^{2+}) octahedra with a short cation-cation distance of ~2.9 Å across the edges (*19*). The *d* electron repulsion across this shared edge may contribute to the relative incompressibility of Fe-rich silicate spinels compared to the dynamics of the smaller Mg end member. The presence of Fe^{3+} in the Fe_{60} and Fe_{78} samples may also increase their bulk moduli, which fall above a linear trend of bulk modulus versus composition as defined by the Mg and Fe values.

The anomalous trend of compressibility versus composition in Mg-Fe silicate spinels points to a fundamental change in the relative behavior of Fe^{2+} and Mg with increasing pressure. At crustal conditions, Mg and Fe^{2+} mimic each other in their crystal chemical roles in oxides and silicates. However, at pressures above 10 GPa their behavior is different.

At low pressure the majority of ferromagnesian silicates, including all rock-forming orthosilicates, chain silicates, and layer silicates with octahedral Fe^{2+} and Mg, form continuous solid solutions and show almost complete octahedral site disorder between Mg and Fe^{2+}. However, three of the most important high-pressure Mg-Fe silicates, wadsleyite β-$(Mg,Fe)_2SiO_4$ and the silicate perovskite and ilmenite forms of $(Mg,Fe)SiO_3$, show only limited Mg-Fe solid solution (*20*). Furthermore, recent crystallographic examination of intermediate high-pressure Mg-Fe phases reveals unusual degrees of Mg-Fe ordering, even in crystals rapidly quenched from temperatures above 1000°C. Significant Mg-Fe ordering has been documented in high-pressure samples of olivine (*21*), wadsleyite (*22*), and anhydrous phase B (*23*). High-pressure ordered olivine is particularly unusual because crustal olivines appear relatively disordered, even from slowly cooled environments (*21, 24*).

The distinction between the high-pressure crystal chemistries of Fe and Mg is further highlighted by the strong intercrystalline separation of these elements between phases at deep-earth conditions. The transition from $(Mg,Fe)_2SiO_4$ silicate spinel to $(Mg,Fe)SiO_3$ perovskite and (Mg,Fe)O magnesiowüstite, which defines the 670-km seismic discontinuity, is characterized by strong partitioning of Fe^{2+} into the oxide phase (*4, 20*). If the contrast between Fe and Mg increases toward the metallic Fe core, it could have significant implications for the compositions and properties of minerals deep in the lower mantle.

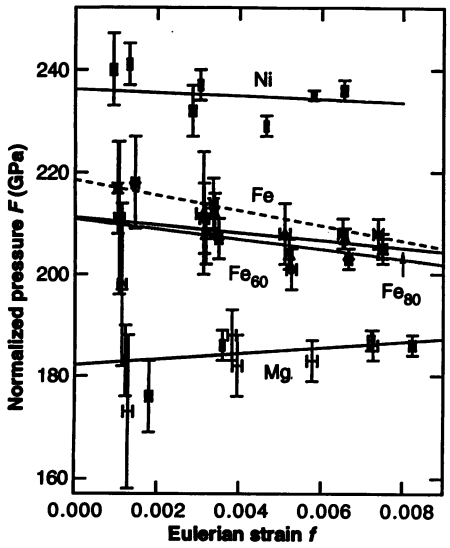

Fig. 3. A plot of Eulerian strain, *f*, versus Birch's normalized stress, *F*, for five silicate spinel compositions to provide equation-of-state information. Lines are weighted linear regression fits to *F-f* data. The zero-pressure bulk modulus is given by the *F*-axis intercept, whereas the deviation of the slope from zero corresponds to the deviation of *K'* from 4. These data demonstrate that compositions rich in Fe are significantly less compressible than the Mg end member. Furthermore, Mg silicate spinel has *K'* >4, whereas Fe-rich compositions have *K'* <4.

REFERENCES AND NOTES

1. P. W. Bridgman, *Proc. Am. Acad. Arts Sci.* **58**, 165 (1923).
2. O. L. Anderson and J. E. Nafe, *J. Geophys. Res.* **70**, 3951 (1965); D. L. Anderson and O. L. Anderson, *ibid.* **75**, 3494 (1970).
3. R. M. Hazen and L. W. Finger, *ibid.* **84**, 6723 (1979).
4. R. Jeanloz and A. B. Thompson, *Rev. Geophys. Space Phys.* **21**, 51 (1983); J. Ita and L. Stixrude, *Eos* **72**, 281 (1991).
5. Support for compositional homogeneity across the 670-km seismic feature is provided by M. S. T. Bukowinski and G. Wolf [*J. Geophys. Res.* **95**, 12583 (1990)] and by Y. Wang *et al.* [*Science* **251**, 410 (1991)].
6. D. L. Anderson and J. D. Bass [*Nature* **320**, 321 (1986)]; E. Knittle, R. Jeanloz, and G. L. Smith [*ibid.* **319**, 214 (1986)]; and L. Stixrude, R. J. Hemley, Y. Fei, and H. K. Mao [*Science* **257**, 1099 (1992)] are among those who argue for a compositionally stratified mantle.
7. R. Shannon, *Acta Crystallogr. A* **32**, 751 (1976).
8. R. M. Hazen and R. Jeanloz, *Rev. Geophys. Space Phys.* **22**, 37 (1984).
9. D. H. Lindsley, *Rev. Miner.* **3**, L1 (1976).
10. R. M. Hazen, *Carnegie Inst. Washington Yearb.* **80**, 277 (1981); R. J. Angel, R. M. Hazen, T. C. McCormick, C. T. Prewitt, J. R. Smyth, *Phys. Chem. Miner.* **15**, 313 (1988); T. C. McCormick, R. M. Hazen, R. J. Angel, *Am. Miner.* **74**, 1287 (1989).
11. R. M. Hazen, J. Zhang, J. Ko, *Phys. Chem. Miner.* **17**, 416 (1990).
12. L. W. Finger, R. M. Hazen, T. Yagi, *Am. Miner.* **64**, 1002 (1979).
13. J. D. Bass, D. J. Weidner, N. Hamaya, M. Ozima, S. Akimoto, *Phys. Chem. Miner.* **10**, 261 (1984).
14. D. J. Weidner, H. Sawamoto, S. Sasaki, M. Kumazawa, *J. Geophys. Res.* **89**, 7852 (1984); R. L. Meng, Y. Fei, D. J. Weidner, personal communication.
15. C. R. Ross II, T. Armbruster, D. Canil, *Am. Miner.* **77**, 507 (1992).
16. I used a Merrill-Bassett diamond-anvil cell [L. Merrill and U. A. Bassett, *Rev. Sci. Instrum.* **45**, 290 (1974)] with 0.75-mm anvil faces, an Inconel 750X gasket (International Nickel, Inc., Toronto, Canada) with a hole 0.50 mm in diameter, and a 4:1 methanol:ethanol pressure fluid. Ruby chips provided an internal pressure calibration, as described by R. M. Hazen and L. W. Finger [*Comparative Crystal Chemistry* (Wiley, New York, 1982)]. Mounting multiple crystals requires one to trade off between larger crystals (which yield more accurate unit-cell parameters) and higher pressures (from gasket deformation). The first mount failed at 3.28 GPa when the 60-μm-thick Mg_2SiO_4 crystal broke into two smaller pieces. The second mount, with a gasket hole of 0.45 mm in diameter and crystals no more than 45 μm thick, was stable to 4.79 GPa, the highest pressure I have obtained with a six-crystal mount.
17. I determined unit-cell parameters on an automated four-circle diffractometer by centering up to 24 reflections from each crystal ($28° < 2\Theta < 50°$) at eight positions, as described by W. C. Hamilton [in *International Tables for X-Ray Crystallography*, J. A. Ebers and W. C. Hamilton, Eds. (Kynoch, Birmingham, U.K., 1974), vol. 4] and adapted for high-pressure studies by H. King and L. W. Finger [*J. Appl. Crystallogr.* **12**, 374 (1979)].
18. R. Jeanloz and R. M. Hazen, *Am. Miner.* **76**, 1765 (1991).
19. B. Kamb, *ibid.* **53**, 1439 (1968). More typical Fe-Fe distances across shared octahedral edges are 3.2 Å in Fe_2SiO_4 olivine and 3.0 Å in FeO.
20. Y. Fei, H.-K. Mao, B. O. Mysen, *J. Geophys. Res.* **96**, 2196 (1991).
21. N. Aikawa, M. Kumazawa, M. Tokonami, *Phys. Chem. Miner.* **12**, 1 (1985).
22. L. W. Finger, R. M. Hazen, J. Zhang, J. Ko, A. Navrotsky, *ibid.*, in press.
23. R. M. Hazen, L. W. Finger, J. Ko, *Am. Miner.* **77**, 217 (1992).
24. G. E. Brown, Jr., *Rev. Miner.* **5**, 275 (1982); J. Stanek, S. S. Hafner, J. A. Sawicki, *Am. Miner.* **71**, 127 (1986); T. Motoyama and T. Matsumoto, *Miner. J.* **14**, 338 (1989).
25. N. L. Ross and R. J. Reeder, *Am. Miner.* **77**, 412 (1992).
26. D. J. Weidner, H. Wang, J. Ito, *Phys. Earth Planet. Inter.* **17**, P7 (1978).
27. J. D. Bass and D. J. Weidner, *J. Geophys. Res.* **89**, 4359 (1984).
28. L. Levien, D. J. Weidner, C. T. Prewitt, *Phys. Chem. Miner.* **4**, 105 (1979).
29. J. Kandelin and D. J. Weidner, *J. Geophys. Res.* **93**, 1063 (1988).
30. These values are from a comparative compressibility study of grospydite garnets now in progress. See also J. D. Bass, *ibid.* **94**, 7621 (1989).
31. D. H. Chang and G. R. Barsch, *ibid.* **78**, 2418 (1973); A. Yoneda, *J. Phys. Earth* **38**, 19 (1990).
32. H. Wang and G. Simmons, *J. Geophys. Res.* **77**, 4379 (1972).
33. E. K. Graham and G. R. Barsch, *ibid.* **74**, 5949 (1969); M. Kumazawa and O. L. Anderson, *ibid.*, p. 5961.
34. J. D. Bass, *Eos* **70**, 474 (1989).
35. J. R. Smyth and D. L. Bish, *Crystal Structures and Cation Sites of the Rock-Forming Minerals* (Allen and Unwin, London, 1988).

36. Crystals were synthesized at the Institute for Solid State Physics, University of Tokyo, by T. Yagi or at the Center for High-Pressure Research, State University of New York (SUNY) at Stony Brook, by J. Ko or D. Weidner.
37. I thank J. Ko, D. J. Weidner, and T. Yagi for the silicate spinel single crystals used in this study and Y. Fei (who also provided Mössbauer analysis of the Fe-bearing samples), C. Meade, and C. Prewitt for valuable discussion and reviews of the manuscript. L. W. Finger and R. J. Angel devised improved operating procedures for the four-circle diffractometer.

3 September 1992; accepted 4 November 1992